

COSMIC RAY PARALLEL AND PERPENDICULAR TRANSPORT IN TURBULENT MAGNETIC FIELDS

SIYAO XU^{1,2} AND HUIRONG YAN¹

Draft version April 3, 2020

ABSTRACT

A correct description of cosmic ray (CR) diffusion in turbulent plasma is essential for many astrophysical and heliospheric problems. This paper aims at presenting physical diffusion behavior of CRs in actual turbulent magnetic fields, model of which has been numerically tested. We perform test particle simulations in compressible magnetohydrodynamic (MHD) turbulence. We obtain scattering and spatial diffusion coefficients by tracing particle trajectories. We find no resonance gap for pitch-angle scattering at 90° . Our result confirms the dominance of mirror interaction with compressible modes for most pitch angles as revealed by the non-linear theory. For cross field transport, our results are consistent with normal diffusion predicted earlier for large scales. The diffusion behavior strongly depends on the Alfvénic Mach number and particle's parallel mean free path. We for the first time numerically derive the dependence of M_A^4 for perpendicular diffusion coefficient with respect to the mean magnetic field. We conclude that CR diffusion coefficients are anisotropic in sub-Alfvénic turbulence and spatially correlated to the local turbulence properties. On scales smaller than the injection scale, we find that CRs are superdiffusive. We emphasize the importance of our results in a wide range of astrophysical processes, including magnetic reconnection.

Subject headings: diffusion–cosmic rays–magnetohydrodynamics (MHD)–turbulence

1. INTRODUCTION

Astrophysical plasma is generally turbulent due to the large spatial scales involved. Propagation of CRs in turbulent magnetic fields plays a key role in understanding many important issues both in space and astrophysics, e.g., solar modulation of CRs, CR acceleration, positron transport, CR anisotropy and diffuse γ -ray emission of the Galaxy (see Jokipii & Parker 1969). However, CR diffusion in turbulent medium is still not fully understood. Current models on CR propagation are often developed by fitting observational data. The conventionally used assumption is that CR diffusion is isotropic and spatially homogeneous, but this too simplified assumption faces major problems in interpreting observations. In addition to the conventional problems, such as the ratio of the boron to carbon, mounting observation evidences challenge the traditional models of propagation. Examples include the spectral hardening at ~ 200 GeV as reported by PAMELA (Adriani et al. 2011) and CREAM (Ahn et al. 2010), inconsistency between the EGRET data and locally measured spectra of CRs (Strong et al. 2004), diffuse γ -ray excess in the inner Galaxy (Ackermann et al. 2012), etc. All these observations imply that a spatially dependent diffusion may hold the key.

CR diffusion depends on the turbulent magnetic fields adopted. Recent advances in turbulence studies necessitate corresponding revisions in CR transport theory. As revealed earlier, CR transport in tested models of turbulence is very different from earlier pictures (Yan & Lazarian 2002, 2004, 2008, hereafter YL02, YL04 and YL08, respectively). In this paper, we shall study numerically the transport of CRs in tested model of turbulence (Goldreich & Sridhar 1995, henceforth GS95; Cho & Lazarian 2003). We employ realistic turbulent magnetic fields, directly produced by three-

dimensional MHD simulations, to provide a reliable description of the diffusion process of CRs. In particular, we shall use compressible MHD turbulence as our input for the following reasons. First of all, turbulence in nature is compressible with finite plasma $\beta \equiv P_{gas}/P_{mag}$. The magnetic pressure P_{mag} cannot be neglected compared to gas pressure P_{gas} for most of the medium that CRs propagate in³. Second of all, the compressible modes, in particular fast magnetosonic modes, have been identified as the most important for CR scattering by both quasilinear theory (YL02, 04) and nonlinear theory (YL08). Indeed pseudo-Alfvén modes (the incompressible limit of slow modes) can contribute through the mirror interactions. This process, however, does not function for particles with small pitch angles (YL08).

Perpendicular transport is another issue that we shall concentrate on in this paper. Many astrophysical environments including heliosphere and our Galaxy have well defined mean magnetic field. In spite of its fundamental importance, cross field transport remains an open question. A popular concept of CR cross field transport is subdiffusion (Kóta & Jokipii 2000; Getmantsev 1963; Mace et al. 2000; Qin et al. 2002; Webb et al. 2006). But it fails to reproduce the diffusion process of solar energetic particles observed in the heliosphere (Perri & Zimbardo 2009). The solar energetic particle fluxes measured at different heliocentric distances indicate a faster diffusion process perpendicular to the solar magnetic field than subdiffusion (MacLennan et al. 2001). Moreover, recent studies based on the tested GS95 model of turbulence have shown that subdiffusion does not apply and instead CR cross field transport is diffusive on large scales and superdiffusive on small scales (YL08; Yan 2013).

In this work, we will focus on investigating the diffusion process of CRs based on the tested model of turbulence. The structure of the paper is as follows. In Section 2, we describe the turbulent magnetic fields we use. In Section 3, we perform

¹ Kavli Institute of Astronomy and Astrophysics, Peking University, Beijing 100871, P.R.China; hryan@pku.edu.cn

² Department of Astronomy, School of Physics, Peking University, Beijing 100871, P.R.China; syxu@pku.edu.cn

³ Otherwise without magnetic field the CRs' propagation will be ballistic, which is against what we know from observations.

test particle simulations in the generated magnetic fields. We investigate particle scattering and parallel diffusion processes in Section 4. In Section 5&6, we present the results on particle perpendicular diffusion behavior, followed by discussions and summary in Section 7&8.

2. GENERATION OF TURBULENT MAGNETIC FIELDS

We use the Cho & Lazarian (2002) code to generate isothermal compressible MHD turbulence at 512^3 resolution. The turbulence evolves on a Cartesian grid with mean magnetic field along the x-direction and the energy injection scale L equal to 0.4 cube size. The total magnetic field is a sum of a uniform background component and a fluctuating component. By varying the input parameters, we derive a data set of MHD turbulence in Fourier space with different Alfvénic Mach numbers. The Alfvénic Mach number is

$$M_A \equiv \langle |\mathbf{v}|/v_A \rangle, \quad (1)$$

where \mathbf{v} is the local velocity, $v_A = |\mathbf{B}|/\sqrt{\rho}$ is the Alfvénic velocity, \mathbf{B} is the local magnetic field, and ρ is density. Here $\langle \dots \rangle$ means a spatially averaged value over all grid points.

M_A describes the perturbation strength of the turbulence with respect to the mean field, and is the single parameter that characterizes the magnetic fields we use. Next we divide our data into sub-Alfvénic ($M_A < 1$) and super-Alfvénic ($M_A > 1$) turbulence for the following simulations.

3. TEST PARTICLE SIMULATIONS

We then trace the trajectories of CRs, in the test particle simulations. Since the relativistic particles have speed much larger than the Alfvén speed, the magnetic field can be treated as stationary and the electric field in the turbulent plasma can be safely neglected for the study of the transport of CRs. We use the Bulirsch-Stoer method (Press et al. 1986) to trace the trajectories of test particles. The algorithm uses an adaptive time-step method and the particle energy is conserved to a high degree during the simulation.

In each time step, the magnetic fields defined on grid points are interpolated to the position of a test particle using a cubic spline routine. Given the local magnetic field \mathbf{B} , the trajectory can be computed by integrating the Lorentz force on each particle,

$$\frac{d\mathbf{u}}{dt} = \frac{q}{mc} \mathbf{u} \times \mathbf{B}, \quad (2)$$

where \mathbf{u} is the particle's velocity and the remaining symbols have their standard meanings. We also use periodic box boundary conditions to keep the number of test particles unchanged.

In each simulation, we release 1000 test particles with random initial positions and pitch angles through the simulation cube. The particle energy is represented by its Larmor radius, expressed as

$$r_L = \frac{u}{\Omega}. \quad (3)$$

Here Ω is the frequency of a particle's gyromotion,

$$\Omega = \frac{eB}{\gamma mc}, \quad (4)$$

where γ is the particle gamma-factor.

Fig. 1(a) and 1(b) show sample particle trajectories in three-dimensional turbulent magnetic fields with different M_A . Obviously, particle diffusion strongly depends on the properties of the turbulence.

4. PITCH-ANGLE SCATTERING AND PARALLEL DIFFUSION

We perform the scattering experiments using an ensemble of particles with a specific pitch angle at the starting point. During the scattering process, the pitch angle, i.e. the angle between the particle's velocity vector and the local magnetic field direction, changes with time. We trace the change of the pitch-angle cosine ($\mu - \mu_0$) in a short time interval to keep the deviation of μ small (see Beresnyak et al. 2011), and obtain pitch-angle diffusion coefficient $D_{\mu\mu}$ by using the definition,

$$D_{\mu\mu} = \frac{\langle (\mu - \mu_0)^2 \rangle}{2t}, \quad (5)$$

averaged over the ensemble of particles. Here μ_0 and μ are the initial and final pitch-angle cosine respectively, and t is the integration time. Fig. 2 displays the calculated $D_{\mu\mu}$ for particles with the same energy, $r_L = 10^{-2}$ cube size and different μ_0 in the turbulence with $M_A = 0.54$. The fitting $D_{\mu\mu}$ curve smoothly extends from $\mu_0 = 0$ to $\mu_0 \sim 1$. Particles with a wide range of pitch angles, including 90° , are scattered due to the resonance broadening, in contrast to the quasilinear theory results. In quasilinear theory, mirror resonance has a sharp peak at large pitch angles close to 90° , but is zero at 90° because of the discrete resonant Landau resonance condition $k_{\parallel} u_{\parallel} = kv_A$, where k_{\parallel} is the component of the wavevector \mathbf{k} parallel to the mean magnetic field, and u_{\parallel} is the parallel velocity component of a particle. In the mean time, gyroresonance also does not function at 90° according to its resonance condition. In nonlinear theory, nonetheless, the small gap around 90° disappears because of the resonance broadening. It is clear from Fig. 2 that our result is consistent with the prediction of the nonlinear theory in YL08. Their analytical calculations show that mirror interaction dominates for large pitch angles till 90° .

The pitch-angle scattering determines the diffusion of CRs parallel to the magnetic field. By substituting $D_{\mu\mu}$ we measured into the equation (Earl 1974)

$$\frac{\lambda_{\parallel}}{L} = \frac{3}{4} \int_0^1 d\mu_0 \frac{u(1 - \mu_0^2)^2}{D_{\mu\mu} L}, \quad (6)$$

where u is particles' velocity, we can obtain the corresponding parallel mean free path of particles. For instance, the corresponding mean free path is $\lambda_{\parallel} = 1.16$ in cube size units for the case considered in Fig. 2.

To measure the parallel diffusion coefficient, we trace the particles over a long distance until we find that they enter the normal diffusion regime, i.e.,

$$\langle (x - x_0)^2 \rangle \propto t. \quad (7)$$

$(x - x_0)$ is the distance measured parallel to the local magnetic field, and then we take the averaged square distance over all particles. The diffusion coefficient is calculated following the definition (Giacomini & Jokipii 1999),

$$D_{\parallel} = \frac{\langle (x - x_0)^2 \rangle}{2t}. \quad (8)$$

Given the parallel diffusion coefficient, we first compute the parallel mean free path λ_{\parallel} of particles directly from D_{\parallel} using the relation

$$\lambda_{\parallel} = \frac{3D_{\parallel}}{u}. \quad (9)$$

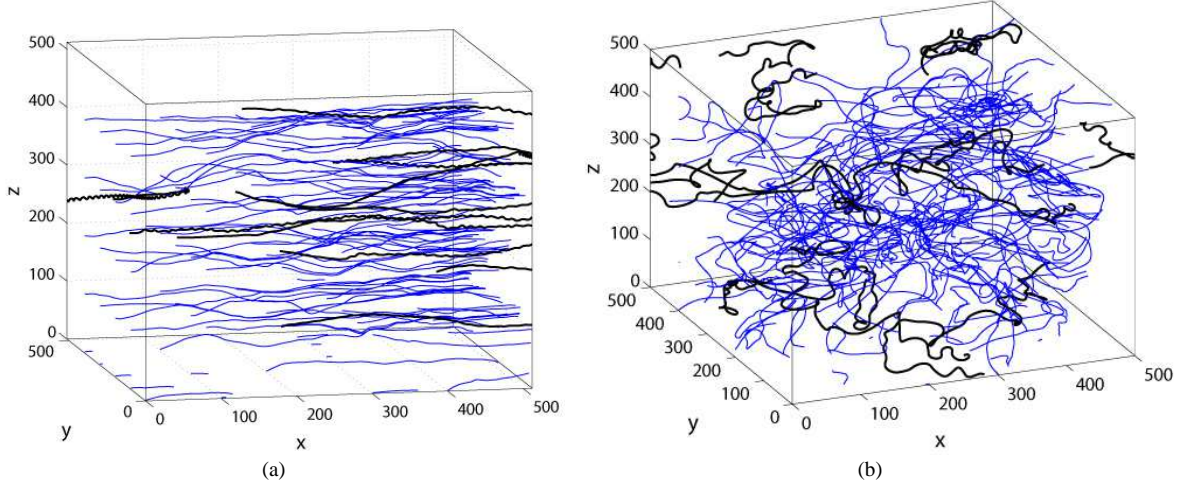


FIG. 1.— Particle trajectories (thick black lines) in (a) sub-Alfvénic turbulence with $M_A = 0.3$ and (b) super-Alfvénic turbulence with $M_A = 1.5$. The thin blue lines display the magnetic field stream lines.

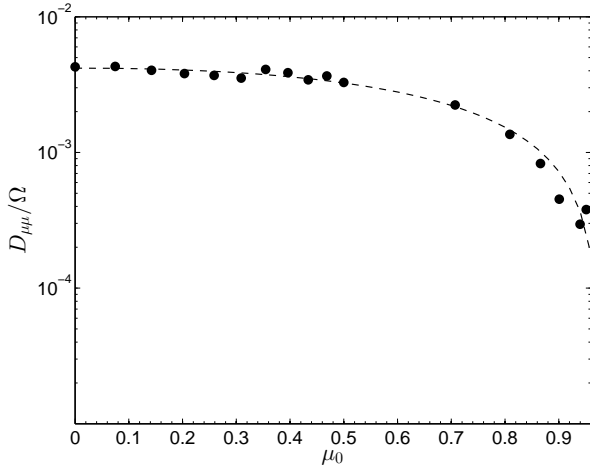


FIG. 2.— Scattering coefficients (filled circles) measured for different initial pitch angles. The numerical results are fitted with a smooth curve (dashed line).

Another method is more straightforward. Since λ_{\parallel} corresponds to the average distance over which the particles undergo 90° scattering, we can derive λ_{\parallel} by tracing the evolution of each particle's pitch angle. Fig. 3 displays the resulting λ_{\parallel} through the two approaches. They show a high consistency with each other. Also, the results are consistent with λ_{\parallel} deduced from $D_{\mu\mu}$ using Eq. (6) (see Fig. 3).

λ_{\parallel} decreases with M_A , showing the increased M_A leads to an enhanced efficiency in particle scattering.

5. CR PERPENDICULAR TRANSPORT ON LARGE SCALES

Since the properties of CR perpendicular diffusion strongly depend on the scale, namely, whether it is larger or smaller than the correlation length of turbulence L , we consider space diffusion separately on large and small scales.

On large scales, similar to the parallel diffusion we described above, we have

$$\langle (y - y_0)^2 \rangle \propto t, \quad (10)$$

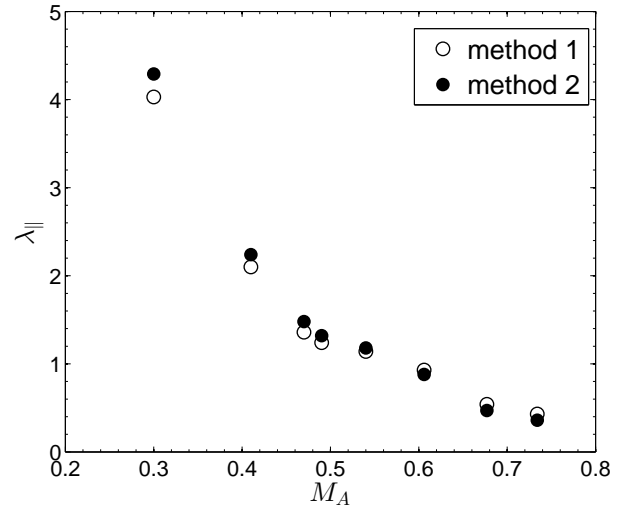


FIG. 3.— λ_{\parallel} (in cube size units) as a function of M_A . λ_{\parallel} values are deduced from D_{\parallel} (open circles) and pitch-angle measurements (filled circles) respectively.

where $(y - y_0)$ represents the perpendicular distance, and

$$D_{\perp} = \frac{\langle (y - y_0)^2 \rangle}{2t}. \quad (11)$$

Note that the perpendicular diffusion coefficient D_{\perp} is calculated across the average magnetic field in the global frame of reference.

For the super-Alfvénic turbulence, it is straightforward to see that the transport is isotropic with a uniform diffusion coefficient since there is no mean magnetic field. Thus we focus on the sub-Alfvénic turbulence ($M_A < 1$).

5.1. $M_A < 1, \lambda_{\parallel} > L$

We consider first the case of $\lambda_{\parallel} > L$, for instance, the cases of ultra high energy CRs and the transport of high energy Galactic CRs in small scale interplanetary turbulence. We measure the perpendicular diffusion coefficients of particles propagating in sub-Alfvénic turbulence with different M_A . Fig. 4 presents D_{\perp} of particles with $r_L = 0.01$ cube size as a function of M_A . The results can be fitted by a line

with a slope of ≈ 3.76 , indicating

$$D_{\perp} \propto M_A^{3.76 \pm 0.52}, \quad (12)$$

with a 95% confidence level. This relation is consistent with equation (26) in YL08, and confirms the dependence of M_A^4 instead of the M_A^2 scaling in Jokipii (1966). This is exactly due to the anisotropy of the Alfvénic turbulence. In the case of sub-Alfvénic turbulence, the eddies become elongated along the magnetic field from the injection scale of the turbulence (Lazarian 2006; YL08). The result indicates that CR perpendicular diffusion depends strongly on M_A of the turbulence, especially in magnetically dominated environments, e.g., the solar corona.

5.2. $M_A < 1, \lambda_{\parallel} < L$

In the sub-Alfvénic turbulence, the mean free paths of the test particles are large because of low scattering rate (see Fig. 3). Due to the limited inertial range of the current MHD simulations, λ_{\parallel} is larger than the injection scale L even for the particles of lowest energies attainable. To study the regime $\lambda_{\parallel} < L$, applicable to most of the CRs, we add resonant slab fluctuations to the initial turbulent magnetic fields obtained through MHD turbulence simulations. Since the slab component is very efficient in pitch-angle scattering through gyroresonance, λ_{\parallel} can be effectively reduced to values smaller than the injection scale of the turbulence with sufficient amplitude. This addition will not affect the statistical properties of particle transport across the field for the following reasons. First of all, the small scale resonant slab modes are uncorrelated with the original turbulence modes. Moreover, the contribution of slab modes to particle cross field transport is sub-diffusive (see Kóta & Jokipii 2000) and therefore can be neglected.

Following the method described above, we measure both D_{\parallel} and D_{\perp} in the composite turbulence. Fig. 5 shows the ratio D_{\perp}/D_{\parallel} for particles with $r_L = 0.01$ cube size as a function of M_A . By fitting to data, we derive

$$\frac{D_{\perp}}{D_{\parallel}} \propto M_A^{3.91 \pm 0.58}, \quad (13)$$

with a 95% confidence level. Our simulation result in this case also agrees with the prediction in YL08.

6. PERPENDICULAR TRANSPORT ON SMALL SCALES

We next consider the perpendicular transport specifically at scales smaller than the injection scale L . We inject 40 beams of test particles randomly in the simulation cube. There are 20 particles in each beam with initial separations equal to several grids and initial pitch angles equal to 0° . All the particles have the same energy with $r_L = 0.01$ cube size. Since we focus on the diffusion behavior of particles on small scales, we trace the particles before their separations reach L .

Since the particles in the sub-Alfvénic turbulence usually have λ_{\parallel} larger than the injection scale in our simulations (see Section 5.2), we assume that particles move strictly along magnetic field lines during the simulation. We then determine the distance travelled along magnetic field lines by

$$\delta x = u \delta t, \quad (14)$$

where u is a constant velocity derived from the initial Larmor radius, and δt is the corresponding time. Fig. 6(a) and

6(b) display the rms of separations between particle trajectories $\langle (\delta z)^2 \rangle^{1/2} / L$ as a function of the displacement of particles moving along the field $|\delta x|/L$ for super-Alfvénic and sub-Alfvénic cases. The separation grows as distance along the field lines to the 1.5 power after passing the minimum perpendicular scale of eddies $l_{\perp, \min}$, up to the injection scale of the strong MHD turbulence ($l_A = L/M_A^3$ for $M_A > 1$ and $l_{tr} \sim LM_A^2$ for $M_A < 1$, Lazarian 2006; YL08). Our result is also consistent with earlier studies on the separation of field lines in Lazarian et al. (2004).

Notably, in real astrophysical world, since CRs have r_L much larger than $l_{\perp, \min}$, they always exhibit superdiffusion on scales smaller than L .

Besides the general relation between $\langle (\delta z)^2 \rangle^{1/2}$ and $|\delta x|$ we confirmed, we also consider a specific case with $\lambda_{\parallel} < L$. Fig. 7 displays the rms of separations between particle trajectories as a function of time. For the scales $L > |\delta x| > \lambda_{\parallel}$, our result suggests

$$\langle (\delta z)^2 \rangle^{1/2} \propto t^{0.75}, \quad (15)$$

consistent with YL08 predictions (see equation (30) and (31) in YL08).

Fig. 8 presents the ratio $\frac{\langle (\delta z)^2 \rangle}{|\delta x|^3}$ as a function of M_A . The best fit to the numerical data shows

$$\frac{\langle (\delta z)^2 \rangle}{|\delta x|^3} \propto M_A^{2.58 \pm 0.64} \quad (16)$$

at 95% confidence. Actually, we notice that even for particles with $\lambda_{\parallel} \geq L$, the pitch angles change significantly especially in cases with higher M_A values. The assumption of no pitch-angle scattering may lead to an overestimate of the parallel distances. Thus, we replace u with the parallel particle velocity u_{\parallel} in Eq. (14). We derive the following relation after this correction (also see Fig. 6(b) and Fig. 8),

$$\frac{\langle (\delta z)^2 \rangle}{|\delta x|^3} \propto M_A^{3.84 \pm 0.78} \quad (17)$$

with 95% confidence, in good agreement with the theoretical predictions (Lazarian & Vishniac 1999; YL08).

7. DISCUSSION

The spatially dependent CR diffusion we obtain with physically motivated model of turbulence should help resolve the current observational puzzles in relation to CR propagation in various astrophysical environments. Our conclusions on CR diffusion shed light on non-local observables, like CR anisotropy and galactic γ -ray diffuse emission.

Perpendicular diffusion of CRs across the mean magnetic field has been considered a difficult problem of particle astrophysics for a long time. We for the first time demonstrated numerically that perpendicular transport of CRs depends on M_A^4 of the turbulence. Our numerical results can be used for a wide range of applications. On large scales, our results on perpendicular diffusion can be applied to depict the normal diffusion of energetic particles in heliosphere, with strong observational constraints (MacLennan et al. 2001). On scales smaller than the energy injection scale, the superdiffusive process is important for describing propagation and acceleration of CRs in supernovae shells and shock regions. The superdiffusive transport on small scales we obtained can also naturally

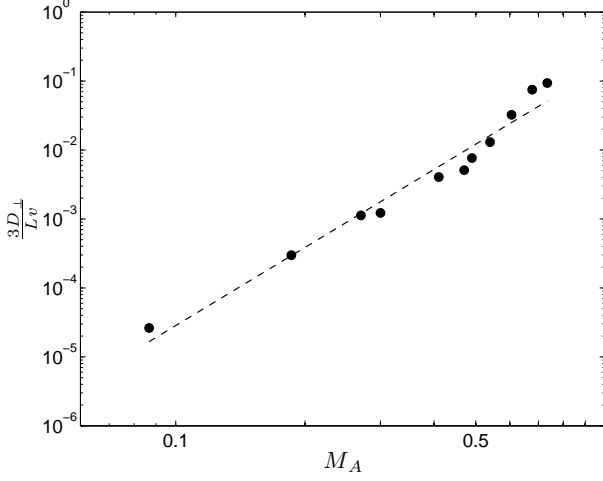


FIG. 4.— D_{\perp} as a function of M_A . The dashed line shows the best fit to the numerical results (filled circles).

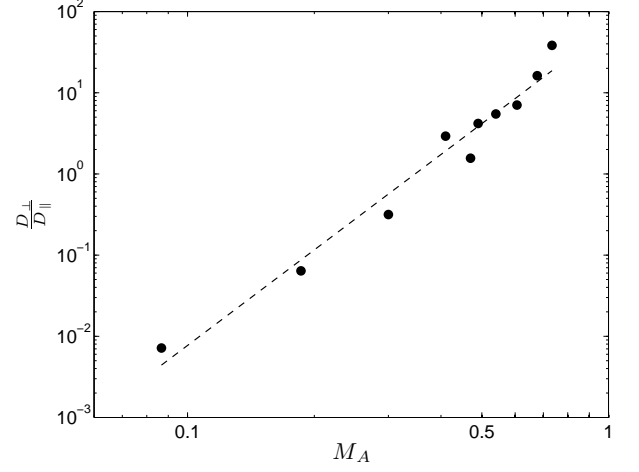
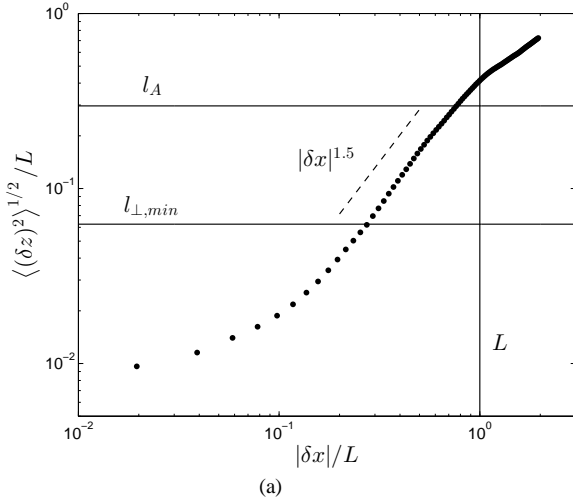
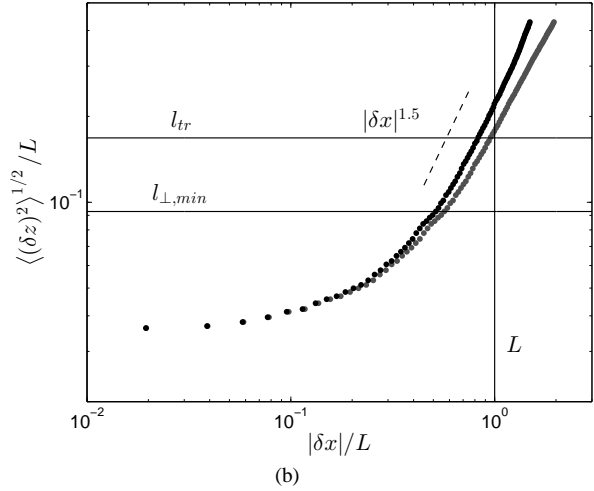


FIG. 5.— Same as Fig. 4 but for $\frac{D_{\perp}}{D_{\parallel}}$.



(a)



(b)

FIG. 6.— $\langle (\delta z)^2 \rangle^{1/2} / L$ vs. $|\delta x| / L$ for (a) $M_A = 1.5$ and (b) $M_A = 0.41$. (b) shows the plots using constant u (lower profile) and u_{\parallel} (upper profile). The dashed line indicates the slope of the curve.

explain the experimental data in heliosphere. For instance, superdiffusion of solar energetic particles has been argued based on the analysis of the particle time profiles (Perri & Zimbardo 2009). They find the propagation of energetic particles in the interplanetary space is superdiffusive.

The feedback of CRs on turbulence, such as gyroresonance instability (see Yan & Lazarian 2011) is not included in the test particle simulations. This shall be a subject of future study.

The diffusion processes we studied in this work have important implications for other issues. Similar diffusion properties and the dependence on M_A can also be applied to thermal particles and our numerical results are consistent with the analytical descriptions in Lazarian (2006). The thermal diffusion has a profound impact on problems such as cooling flows in clusters of galaxies.

As a fundamental astrophysical process, magnetic reconnection is controlled by the turbulent wandering of magnetic field (Lazarian & Vishniac 1999). The diffusion behavior of field lines is essential for determining the reconnection rate in

turbulent medium. The M_A dependence that we for the first time numerically confirmed in this paper can help quantitatively determine the extension degree of the outflow region and the resulting magnetic reconnection rate.

8. SUMMARY

We provide a realistic description of particle transport with test particle simulations in tested model of compressible turbulence.

1. Pitch-angle scattering experiments are consistent with nonlinear theory, showing the dominance of mirror interaction for most of the pitch angles except for small ones.
2. The nonlinear effect for pitch angles close to 90° has been confirmed by our simulations.
3. We have demonstrated numerically that CRs are diffusive on large scales. We show that perpendicular diffusion coefficient depends on M_A^4 in sub-Alfvénic turbulence.

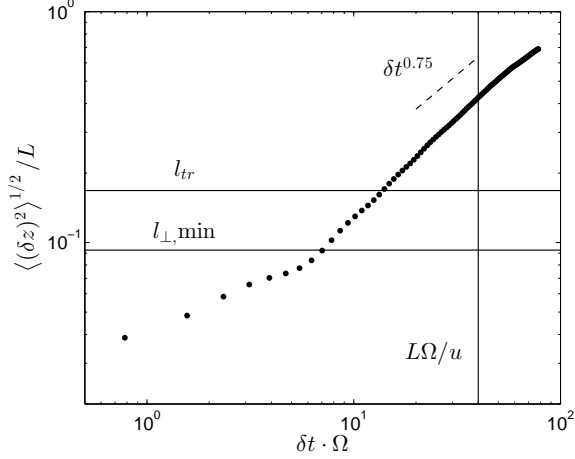


FIG. 7.— $\langle(\delta z)^2\rangle^{1/2}/L$ vs. $\delta t \cdot \Omega$ for $M_A = 0.41$. The dashed line indicates the slope of the curve, and the vertical line denotes the time for particles to travel L .

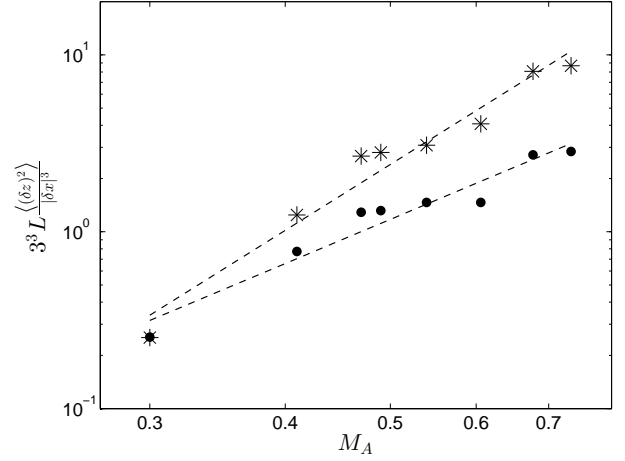


FIG. 8.— $\frac{\langle(\delta z)^2\rangle}{|\delta x|^3}$ as a function of M_A . Filled circles are for previous results with constant velocity, and stars are for results after the correction for u . The dashed lines are the best fits to the data.

4. We confirm that CR diffusion coefficients are anisotropic ($\propto M_A^4$) for $M_A < 1$ as predicted earlier by YL08.
5. On small scales, CRs experience superdiffusion rather than subdiffusion.

SX and HY are supported by NSFC grant AST-11073004. We acknowledge the computing support from FSC-PKU. We thank useful discussions with Blakesley Burkhart.

REFERENCES

- Ackermann, M., et al. 2012, *ApJ*, 750, 3
 Adriani, O., et al. 2011, *Science*, 332, 69
 Ahn, H. S., et al. 2010, *ApJ*, 714, L89
 Beresnyak, A., Yan, H., & Lazarian, A. 2011, *ApJ*, 728, 60
 Cho, J., & Lazarian, A. 2002, *Physical Review Letters*, 88, 245001
 —. 2003, *MNRAS*, 345, 325
 Earl, J. A. 1974, *ApJ*, 193, 231
 Getmantsev, G. G. 1963, *Soviet Ast.*, 6, 477
 Giacalone, J., & Jokipii, J. R. 1999, *ApJ*, 520, 204
 Goldreich, P., & Sridhar, S. 1995, *ApJ*, 438, 763
 Jokipii, J. R. 1966, *ApJ*, 146, 480
 Jokipii, J. R., & Parker, E. N. 1969, *ApJ*, 155, 799
 Kóta, J., & Jokipii, J. R. 2000, *ApJ*, 531, 1067
 Lazarian, A. 2006, *ApJ*, 645, L25
 Lazarian, A., & Vishniac, E. T. 1999, *ApJ*, 517, 700
 Lazarian, A., Vishniac, E. T., & Cho, J. 2004, *ApJ*, 603, 180
 Mace, R. L., Matthaeus, W. H., & Bieber, J. W. 2000, *ApJ*, 538, 192
 MacLennan, C. G., Lanzerotti, L. J., & Hawkins, S. E. 2001, in *International Cosmic Ray Conference*, Vol. 8, *International Cosmic Ray Conference*, 3265
 Perri, S., & Zimbardo, G. 2009, *ApJ*, 693, L118
 Press, W. H., Flannery, B. P., & Teukolsky, S. A. 1986, *Numerical recipes. The art of scientific computing*
 Qin, G., Matthaeus, W. H., & Bieber, J. W. 2002, *ApJ*, 578, L117
 Strong, A. W., Moskalenko, I. V., & Reimer, O. 2004, *ApJ*, 613, 962
 Webb, G. M., Zank, G. P., Kaghshvili, E. K., & le Roux, J. A. 2006, *ApJ*, 651, 211
 Yan, H. 2013, *ArXiv*: 1302.3246
 Yan, H., & Lazarian, A. 2002, *Physical Review Letters*, 89, B1102+
 —. 2004, *ApJ*, 614, 757
 —. 2008, *ApJ*, 673, 942
 —. 2011, *ApJ*, 731, 35